SCALAR TRANSPORT MODELLING OF TURBULENT JET DIFFUSION FLAMES

Wai-Tung Chan and Yang Zhang
Thermodynamics and Fluid Mechanics Division
Mechanical Engineering Department
UMIST
PO BOX 88, Manchester, M60 1QD, U.K.

ABSTRACT

This paper focuses on the scalar flux modelling in the predictions of turbulent jet diffusion flames. Recently, full non-linear second-moment closure modelling approach (model which include non-linear effects for pressure-strain and pressure-scalar correlations), that guarantee realizability constraint and a two-component limit, has been applied for diffusion flames. It has been demonstrated to be particularly beneficial for flame predictions especially on the prediction of scalar transport. Systematic tests are being carried out to assess its advantages and disadvantages over other simpler models. Two methane jet flames have been chosen for the current study.

INTRODUCTION

Eddy viscosity concept together with a simple, one-step, global reaction model is widely used over the years and maintained its popularity due to its simplicity and success on some simple turbulent reacting flow predictions. The combined model provided reasonable approximations on mean properties such as velocity, mixture fraction and temperature along the axis. However fluctuation properties as well as the radial profile of the mean temperature were normally predicted incorrectly. Due to the complex natural of practical combusting systems, a more appropriate turbulence model is necessary in order to take into account of the effect of swirl, recirculation and wall. Further effort on turbulence modelling is essential in order to achieve high prediction accuracy of a reacting system.

The shortcomings of the eddy viscosity have led to an interest on the practicality of second-moment closures (SMCs). Schneider and Janicka (1990) performed a SMC prediction, which takes into account of the Reynolds-number dependence, on methane-air diffusion flame. Their results show that the hydrodynamic field is well predicted in the upstream region (X/D<15) but not in the downstream region. Despite there is no comparisons between the experimental results and predictions on the scalar field, their paper shows that the prediction of the spreading rate of the flame and the turbulent stresses remains to be the major problems in turbulence modelling. The drawback of the SMC related to the existence of the round jet anomaly and its improvements can be found in Craft (1991). Craft proposed a pressure-scalar gradient correlation model, which includes terms up to cubic order in second-moment quantities, together with a cubic order pressure-strain model for isothermal flow predictions. Better predictions on the scalar fluxes are particularly found. Recently Chan and Zhang (1999) applied this cubic modelling approach on various jet diffusion flames. The results are encouraging. Jones (1994) demonstrated the superiority of SMC in the predictions of isothermal jet flows and a turbulent propane flame. The characteristics of those flows are being predicted reasonably well despite there are some deviations on the fluctuating properties compared with the experimental data. More recently Jones and Kakhi (1997) performed predictions of hydrocarbon-air turbulent jet diffusion flames using a κ-ε turbulence model and a SMC model to describe the turbulent transport. The scalar field of the flames was represented by a scalar probability density function (PDF) equation which was solved by Monte Carlo simulation. Their studies suggest that the κ-ε turbulence model could reproduce the mean properties very well and hence they argued that more sophisticated turbulence closure coupled to the same simple mixing models might only bring little improvement in the prediction of the reactive scalar field. It is worth of mentioning that this paper intends to have a systematic evaluation of some turbulence models and their effect on combustion.

TEST CASES AND MODELLING APPROACH

Two methane jet flames, labelled as Flame L and Flame M, have been chosen for the current studies. Both flames have been investigated experimentally or computationally (or a combination of both) by Masri et al (1988, 1990) and Chen et al (1989). Flame L has Reynolds number around 20000 whereas Flame M has Reynolds number around 27000. The geometry of the burner for both flames is the same. Both

flames were stabilised and surrounded by a large ring of pilot flames. In the current study all the numerical computations are obtained with the finite volume elliptic solver, a version of the UMIST code TEAM (Huang and Leschziner 1983). Different turbulence models are employed for the hydrodynamic and scalar fields. They are the standard κ-ε turbulence approach (Jones and Launder 1972), the generalised gradient diffusion hypothesis (GGDH) approach (Daly and Harlow 1970), the linear approaches and the cubic approach of SMC. By cubic we mean the non-linear effects in stresses and fluxes are up to third order. The turbulence modelling aspects based on SMCs can be found in the review paper of Launder (1996). However a summary of the turbulence models used is listed in the Appendix. Additional source terms arise in combusting systems have been implemented in the code. Details of the combustion related source terms could be found in Jones (1994). For simplicity, combustion chemistry is described as a global overall one-step reaction. The assumptions of the Shvab-Zeldovich formalism are adopted and laminar flamelet approach for chemical reactions has been applied. The interactions of turbulence and chemical reactions are coupled by presumed β-probability density function (PDF).

RESULTS AND DISCUSSION

The comparison between the experimental date and the predictions of the mean mixture fraction, Z, profiles and the mean temperature, T, profiles for Flame L are shown in Figure 1 and 2. The profiles are plotted along the normalised radial direction, r/D, and against the normalised axial direction, X/D. The inner nozzle diameter, D, is 7.2mm. Three models are compared in the figures. They are the full non-linear SMC, linear SMC and the κ-ε model. In the full non-linear SMC, the pressure-strain and the pressure-scalar correlations appear in the stress equations and the scalar flux equations respectively are approximated by the cubic approaches (Eq. 6 and 7 in Appendix). The time scalar ratio, R, which appears in the pressure-scalar correlation terms, is assumed to be a constant value of two. The scalar dissipation rate ε_z is approximated by Eq. 8. For the κ-ε modelling approach, ε_z is defined as $\varepsilon_z = 2D_z (\partial Z/\partial x_k)^2$. D_z is the common diffusivity. Figure 1 and 2 illustrate the superiority of the cubic SMC over the linear SMC. The linear model underestimates the mixture fraction near the centreline region but overestimates the mixture fraction after the mixing zone. On the temperature profiles, the linear model largely over-predicts the temperature. The discrepancies increase as the X/D increases. By comparing the pressure-scalar correlation modelling approach in both the linear and the cubic model, it is found that terms such as the mean scalar gradient and the anisotropic tensors would have a strong influence on the predictions of the flame. Despite the fact that the κ-ε model has a tendency of over-predicting both the mixture fraction and the mean temperature (after the mixing zone), it also produces comparable results with the cubic SMC.

Figure 3 and 4 show the mixture fraction and the temperature profiles of Flame M. The over-predictions of mixture fraction by the κ-ε model now can be clearly seen.

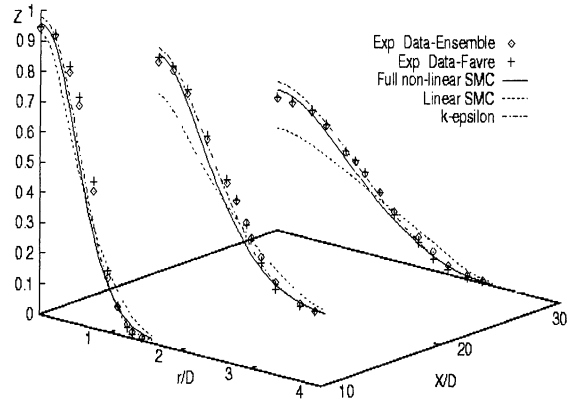

Figure 1. Profiles of mean mixture, Z, of Flame L.

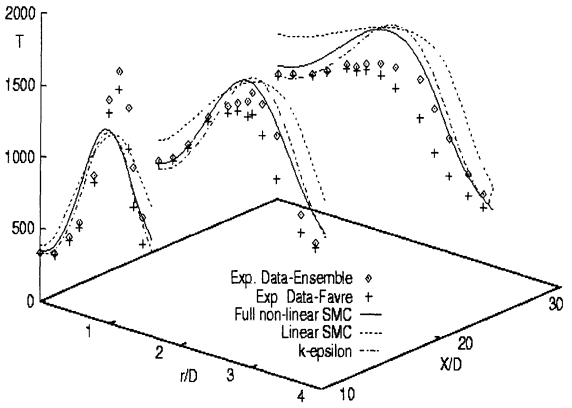

Figure 2. Profiles of mean temperature, T°C, of Flame L.

The temperature profiles computed by the κ-ε model are comparable to the cubic SMC and the centreline values are more accurately predicted. All the models show high temperature deficit for X/D≥20. Masri and Pope (1990) employed joint PDF equation, which is solved by Monte Carlo method. They also confirmed this large temperature disagreement. The discrepancy could be attributed to the high strain rate, which may lead to localized extinction, in the Flame M as suggested by Masri and Pope. The radial profiles of the mixture fraction variance, z'', at different axial locations are plotted in Figure 5. In general all the models perform very well after the mixing zone. The κ-ε model generates very close to zero centreline values, which is in contradict to the experimental results, at all axial locations. Although the SMCs overestimate the centreline values the overall trend and the characteristics of the mixture fraction variance are predicted reasonably well.

In order to demonstrate the overall predictability of all models the mean axial velocity, U, and the stress components, u'' and v'' are shown in Figure 6-8. Since the

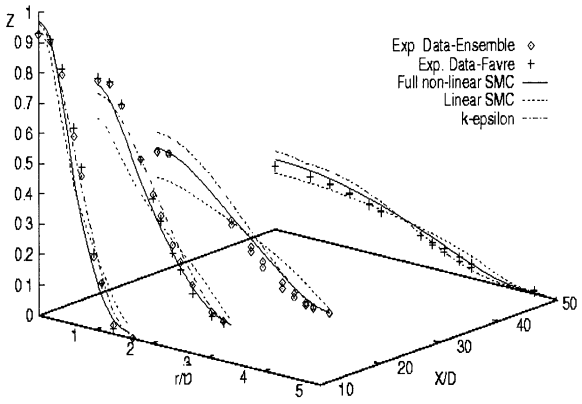

Figure 3. Profiles of mean mixture, Z, of Flame M.

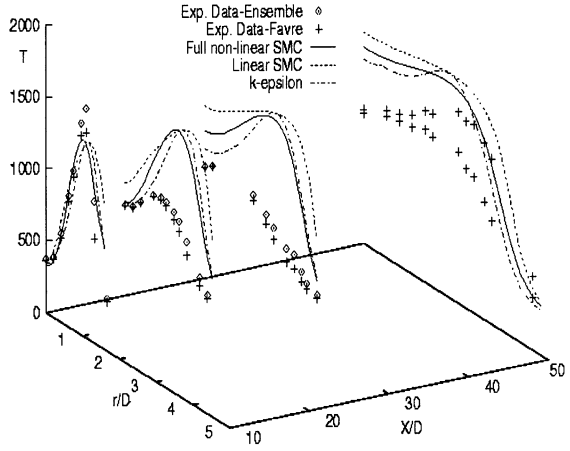

Figure 4. Profiles of mean temperature, T°C, of Flame M.

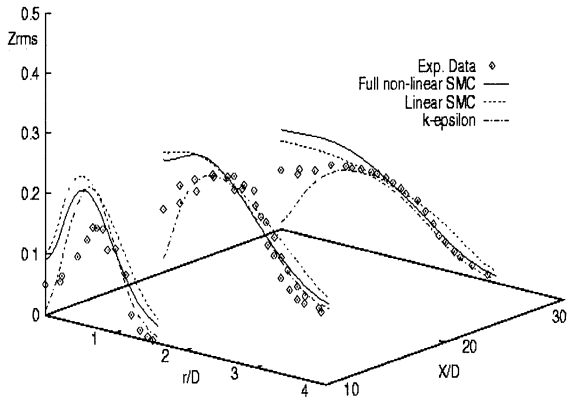

Figure 5. Profiles of mixture fraction variance, z'', of Flame L.

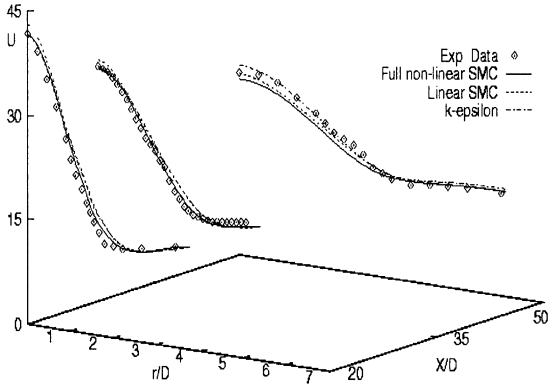

Figure 6. Profiles of mean axial velocity, U ms^{-1}, of Flame L.

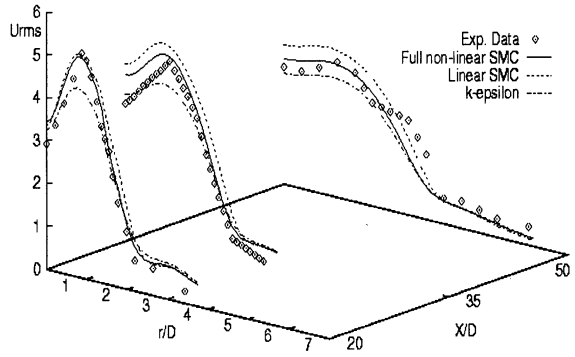

Figure 7. Profiles of streamwise stress component, u'' ms^{-1}, profiles of Flame L.

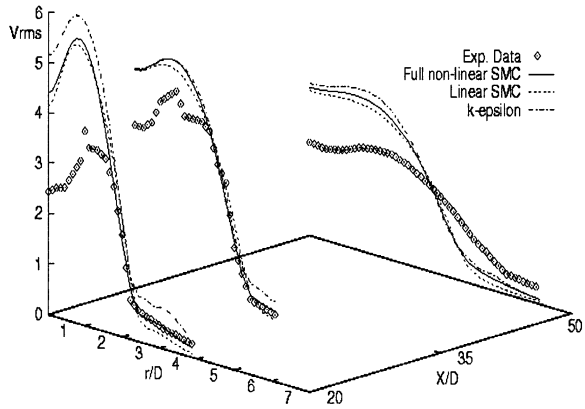

Figure 8. Profiles of normal stress component, v'' ms^{-1}, profiles of Flame M

stresses are obtained through their own transport equations in the SMC approach, the spreading rate is certainly look better than that by the κ-ε model. Also the κ-ε model produces too low peak values of the u'' but relatively high values for the v''. The discrepancies are reduced as X/D increases. This is due to the disappearing of the strong formation of anisotropy close to the nozzle. It is worth of pointing out that both the u'' and v'' are over-predicted at the centreline region by the SMCs, This suggests that the kinetic energy in that region is too strong.

Although there is no experimental data of scalar fluxes available for comparison, we still can come to a conclusion that further improvement in the thermodynamic field is necessary. It is sensible to assume that the prescribed time-scale ratio R (=2) may play a part in the problem. Calculations are therefore performed using a scalar dissipation rate transport equation (Eq. 9) together with the full cubic SMC. Results (not shown here) indicate that Eq. 9 could not remove the discrepancy found in the mixture variance predictions. However the coefficients depended on invariants such as A_2 and A, appeared in the mechanical and scalar time-scales in Eq. 9, could improve the prediction of the mixing layer of the flame. In order to increase the scalar dissipation rate and hence reduce the magnitude of the variance, additional term is included in Eq. 9 as

$$Add = Const.\frac{\varepsilon}{\varepsilon_z}\widetilde{z''^2}\left(\frac{\partial \tilde{Z}}{\partial x_i}\right)^2 \qquad (10)$$

The constant is equal to 0.30 in this study. The results, the profiles of mixture fraction variance for Flame M, are shown in Figure 9. The variance is better described by Eq. 10. The figure also illustrates the predictability of the GGDH modelling approach with the non-linear Reynolds stress model. It is worth of mentioning that the GGDH approach could produce very similar results to the full cubic SMC. This may suggest that, for turbulent combustion calculation with simple flow configuration, the use of GGDH may be advantageous. However in practical combusting systems the GGDH is more likely give wrong predictions (as a non-gradient diffusion is likely to occur and also due to the transport effect of the scalar flux is being ignored). Figure 10 and 11 show the profiles of the mean density and the mean temperature of Flame L respectively using Eq. 10. Slightly more realistic predictions are found. This indicates that the thermal spreading rate of the flame is now described better than before. The density profiles show that current modelling approaches (both the turbulence models and the combustion model) can predict the density value in the fuel-rich region reasonably well. However the size of the region is overestimated. Chen et al (1989) also encountered this problem. They applied a PDF modelling on Flame L using two slightly more complex combustion models (either the five-scalar, four-step, reduced mechanism or the four-scalar constrained equilibrium approach). They claimed that the chemical kinetics is out of equilibrium and this may not be well captured by their combustion models. Also frequent local flame extinction observed in Flame L could contribute to the deficit.

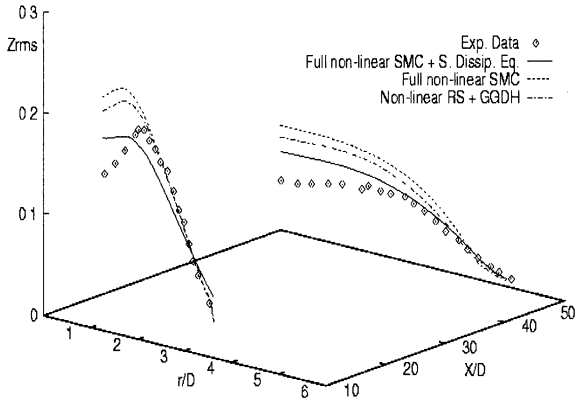

Figure 9. Profiles of mixture fraction variance, z'', of Flame M.

CONCLUSION

Various scalar flux modelling approaches are performed and investigated on the predictions of turbulent jet diffusion flames. Results suggest that the full non-linear, cubic, SMC could predict well on both the hydrodynamic and thermodynamic fields of the flames. The κ-ε model and the GGDH approach in the current test cases also provide comparable results with the cubic model in the prediction of scalar field. However these kind of gradient-transport concept can be erroneous in predicting more complex interactions between the turbulence and the chemistry in a practical combusting system.

In order to obtain better predictions on the scalar variance, a transport equation of the scalar dissipation rate is solved together with a new additional term. Results not only show better predictions can be achieved but also demonstrate the potential of SMCs. Further improvement can be easily made if there are experimental data of scalar fluxes available.

ACKNOWLEDGEMENTS

The Authors would like to thank Dr. T.J. Craft for very helpful discussions and advice. This work was partly supported by EPSRC under the grant number GR/L60722 and a separate EPSRC scholarship to the first author.

REFERENCES

Chan, W.T., and Zhang, Y., 1999, "Modelling Turbulent Diffusion Flames with Full Second-moment Closure using Cubic, Realizable Models," 4th International Symposium on Engineering Turbulence Modelling and Measurements.

Chen, J.Y., Kollmann, W., and Dibble, R.W., 1989, "Pdf modeling of Turbulent Nonpremixed Methane Jet Flames," Sandia Report, SAND89-8403.

Craft, T.J., 1991, "Second-Moment Modelling of Turbulent Scalar Transport," Ph.D. Thesis, Faculty of Technology, Univ. of Manchester.

Daly, B.J., and Harlow, F.H., 1970, "Transport Equations in Turbulence," Phys. Fluids, Vol. 13, pp. 2634-2649.

Huang, P.G., and Leschziner, M.A., 1983, "An Introduction and Guide to the computer code," Dept. Mech. Eng., UMIST. Report TFD/83/9 (R).

Jones, W.P., 1994, "Turbulence Modelling and Numerical Solution Methods for Variable Density and Combusting Flows," Turbulent Reacting Flows, Academic Press, Chapter 6, pp. 309-374.

Jones, W.P., and Kakhi, M., 1997, "Application of the Transported pdf Approach to Hydrocarbon-Air Turbulent Jet Diffusion Flames," Combust. Sci. and Tech., Vol. 129, pp. 393-430.

Jones, W.P., and Launder, B.E., 1972, "The Prediction on Laminarization with a Two-Equation Model of Turbulence," Int. J. Heat Mass Transfer, Vol. 15, pp. 301-314.

Launder, B.E., 1996, "An Introduction to Single-Point Closure Methodology," Lesieur et al., ed., Elsevier Science B.V. Course 6.

Masri, A.R., Bilger, R.W., and Dibble, R.W., 1988, "Conditional Probability Density Functions Measured in Turbulent Nonpremixed Flames of Methane Near Extinction," Combustion and Flame, Vol. 74, pp. 267-284.

Masri, A.R., and Pope, S.B., 1990, "Pdf Calculations of Piloted Turbulent Nonpremixed Flames of Methane," Combustion and Flame, Vol. 81, pp. 13-29.

Schneider, F., and Janicka, J., 1990, "The Reynolds-Stress Tensor in Diffusion Flames An Experimental and Theoretical Investigation," Combustion and Flame, Vol. 81, pp. 1-12.

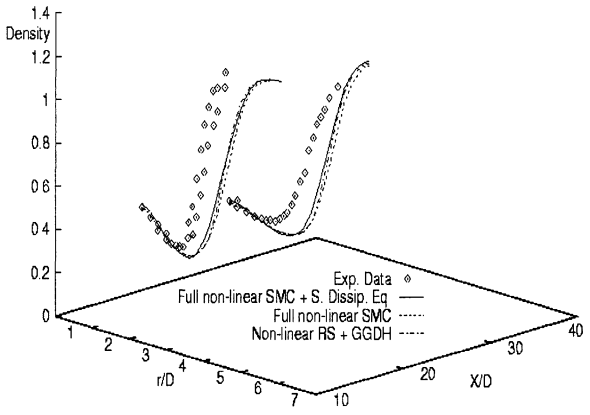

Figure 10. Profiles of mean density, kgm^{-3}, of Flame L.

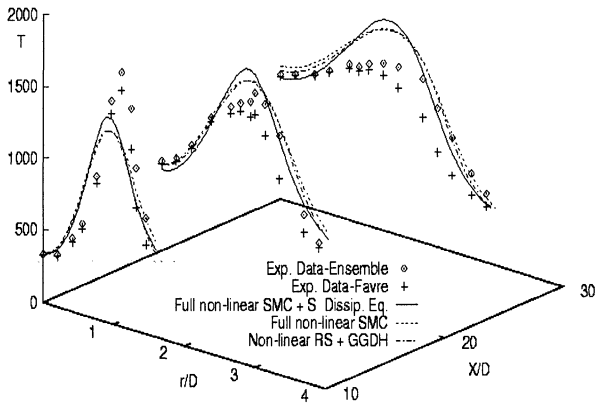

Figure 11. Profiles of mean temperature, T°C, of Flame L.

APPENDIX

The Reynolds stresses and the scalar fluxes in the standard κ-ε turbulence approach are approximated as

$$\overline{\rho}\widetilde{u_i''u_j''} = -\mu_t\left(\frac{\partial \tilde{U}_i}{\partial x_j}+\frac{\partial \tilde{U}_j}{\partial x_i}\right)+\frac{2}{3}\overline{\rho}\delta_{ij}k \tag{1}$$

and

$$\overline{\rho}\widetilde{u_i''z''} = -\frac{\mu_t}{\sigma_z}\frac{\partial \tilde{Z}}{\partial x_i} \tag{2}$$

where

$$\mu_t = 0.09\overline{\rho}\frac{k^2}{\varepsilon} \qquad ; \qquad \sigma_z = 0.9$$

If the GGDH is used, the scalar flux is approximated as

$$\overline{\rho}\widetilde{u_i''z''} = 0.15\overline{\rho}\frac{k}{\varepsilon}\widetilde{u_i''u_k''}\frac{\partial \tilde{Z}}{\partial x_k} \tag{3}$$

In the SMC, the pressure-strain and pressure-scalar correlations are modelled by either the linear approach

$$\begin{aligned}\overline{u_j''\frac{\partial p'}{\partial x_i}}+\overline{u_i''\frac{\partial p'}{\partial x_j}} = \; & 1.8\frac{\varepsilon}{k}\left(\overline{\rho}\widetilde{u_i''u_j''}-\frac{1}{3}\delta_{ij}\overline{\rho}\widetilde{u_k''u_k''}\right)\\ & +0.6\left(P_{ij}-C_{ij}-\frac{1}{3}\delta_{ij}\left(P_{kk}-C_{kk}\right)\right)\end{aligned} \tag{4}$$

where

$$P_{ij} = -\overline{\rho}\left(\widetilde{u_i''u_k''}\frac{\partial \tilde{U}_j}{\partial x_k}+\overline{\rho}\widetilde{u_j''u_k''}\frac{\partial \tilde{U}_i}{\partial x_k}\right)$$

$$C_{ij} = \overline{\rho}\tilde{U}_k\frac{\partial \widetilde{u_i''u_j''}}{\partial x_k}$$

and for the pressure-scalar correlations,

$$\overline{z''\frac{\partial p'}{\partial x_i}} = 3.0\frac{\varepsilon}{k}\widetilde{u_i''z''}-0.5\widetilde{u_k''z''}\frac{\partial \tilde{U}_i}{\partial x_k}-0.5\tilde{U}_k\frac{\partial \widetilde{u_i''z''}}{\partial x_k} \tag{5}$$

Or the non-linear, cubic, approaches

$$\begin{aligned}\overline{u_j''\frac{\partial p'}{\partial x_i}}+\overline{u_i''\frac{\partial p'}{\partial x_j}} = \; & 3.1(A_2A)^{0.5}\varepsilon\left[a_{ij}+1.2\left(a_{ik}a_{jk}-\frac{1}{3}A_2\delta_{ij}\right)\right]\\ & +\varepsilon a_{ij}+0.6\left(P_{ij}-\frac{1}{3}P_{kk}\delta_{ij}\right)-0.3\varepsilon a_{ij}\frac{P_{kk}}{\varepsilon}\\ & +0.2\left[\begin{array}{l}\dfrac{\widetilde{u_k''u_j''}\,\widetilde{u_l''u_i''}}{k}\left(\dfrac{\partial \tilde{U}_k}{\partial x_l}+\dfrac{\partial \tilde{U}_l}{\partial x_k}\right)\\ -\dfrac{\widetilde{u_l''u_k''}}{k}\left(\widetilde{u_i''u_k''}\dfrac{\partial \tilde{U}_j}{\partial x_l}+\widetilde{u_j''u_k''}\dfrac{\partial \tilde{U}_i}{\partial x_k}\right)\end{array}\right]\end{aligned} \tag{6}$$

and for the pressure-scalar correlations reads

$$\begin{aligned}\overline{z''\frac{\partial p'}{\partial x_i}} = \; & 1.7\left(1+1.2(A_2A)^{0.5}\right)R^{0.5}\frac{\varepsilon}{k}\left[\begin{array}{l}\widetilde{u_i''z''}\left(1+0.6A_2\right)\\ -0.8a_{ik}\widetilde{u_k''z''}\\ +1.1a_{ik}a_{kj}\widetilde{u_j''z''}\end{array}\right]\\ & +0.2A^{0.5}Rka_{ij}\frac{\partial \tilde{Z}}{\partial x_j}\\ & -0.8\widetilde{u_k''z''}\frac{\partial \tilde{U}_i}{\partial x_k}+0.2\widetilde{u_k''z''}\frac{\partial \tilde{U}_k}{\partial x_i}-0.165\frac{P_{kk}}{\varepsilon}\widetilde{u_i''z''}\\ & +0.4\widetilde{u_k''z''}a_{il}\left(\frac{\partial \tilde{U}_k}{\partial x_l}+\frac{\partial \tilde{U}_l}{\partial x_k}\right)\\ & -0.1\widetilde{u_k''z''}a_{ik}a_{ml}\left(\frac{\partial \tilde{U}_m}{\partial x_l}+\frac{\partial \tilde{U}_l}{\partial x_m}\right)\\ & +0.1\widetilde{u_k''z''}\left(\frac{a_{im}P_{mk}+2a_{mk}P_{im}}{k}\right)\\ & -0.15a_{ml}\left(\frac{\partial \tilde{U}_k}{\partial x_l}+\frac{\partial \tilde{U}_l}{\partial x_k}\right)\left(a_{mk}\widetilde{u_i''z''}-a_{mi}\widetilde{u_k''z''}\right)\\ & +0.05a_{ml}\left[\begin{array}{l}7a_{ml}\left(\widetilde{u_i''z''}\dfrac{\partial \tilde{U}_k}{\partial x_l}+\widetilde{u_k''z''}\dfrac{\partial \tilde{U}_i}{\partial x_l}\right)\\ -\widetilde{u_k''z''}\left(a_{ml}\dfrac{\partial \tilde{U}_i}{\partial x_k}+a_{mk}\dfrac{\partial \tilde{U}_i}{\partial x_l}\right)\end{array}\right]\end{aligned} \tag{7}$$

where the time scale ratio, R, can be equal to 2 or

$$R = 2\frac{k}{\varepsilon}\frac{\varepsilon_z}{\widetilde{z''^2}} \tag{8}$$

where ε_z can be approximated using its own transport equation

$$\begin{aligned}\frac{d\varepsilon_z}{dt} = \; & \left(-1.6\widetilde{u_k''z''}\frac{\partial \tilde{Z}}{\partial x_k}+2.6\frac{\nu_t}{\varepsilon}\varepsilon_z\left(\frac{\partial \tilde{U}_i}{\partial x_j}\right)^2\right)\frac{\varepsilon}{kR}-\frac{0.9}{1+1.1A_2A^{0.5}}\frac{\varepsilon_z\varepsilon}{k}\\ & -\frac{2}{1+1.1A_2A^{0.5}}\frac{\varepsilon_z^2}{\widetilde{z''^2}}+0.25\frac{\partial}{\partial x_k}\left(\widetilde{u_k''u_l''}\frac{k}{\varepsilon}\frac{\partial \varepsilon_z}{\partial x_l}\right)\end{aligned} \tag{9}$$